




Exosomes derived from HEK293T cells interact in an efficient and noninvasive manner with mammalian sperm *in vitro*

Teresa Vilanova-Perez¹, Celine Jones¹, Stefan Balint², Rebecca Dragovic¹, Michael L Dustin² , Marc Yeste³ & Kevin Coward^{*,1}

¹Nuffield Department of Women's & Reproductive Health, University of Oxford, Level 3, Women's Centre, John Radcliffe Hospital, OX3 9DU, Oxford, UK

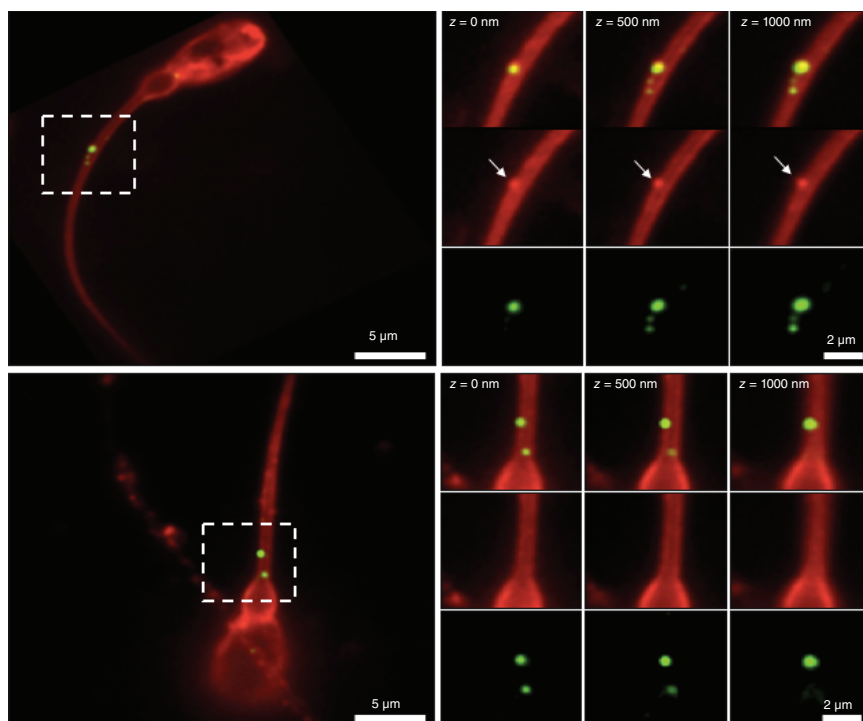
²Nuffield Department of Orthopaedics, The Kennedy Institute of Rheumatology, Rheumatology & Musculoskeletal Sciences, University of Oxford, Roosevelt Drive, Headington, OX3 7FY, Oxford, UK

³Department of Biology, Biotechnology of Animal & Human Reproduction (TechnoSperm), Unit of Cell Biology, Institute of Food & Agricultural Technology, University of Girona, E-17003, Girona, Spain

*Author for correspondence: Tel.: +44(0)1865 618900; Fax: +44(0)1865 769141; kevin.coward@wrh.ox.ac.uk

Aim: To investigate exosomes as a noninvasive delivery tool for mammalian sperm. **Materials & Methods:** Exosomes were isolated from HEK293T cells and co-incubated with boar sperm *in vitro*. **Results:** Internalized exosomes were detected within 10 min of co-incubation. Computer-assisted sperm analysis and flow cytometry demonstrated that even after 5-h of exposure to exosomes, there were no significant deleterious effects with regard to sperm motility, viability, membrane integrity and mitochondrial membrane potential ($p > 0.05$), thus indicating that exosomes did not interfere with basic sperm function. **Conclusion:** HEK293T-derived exosomes interacted with boar sperm without affecting sperm function. Exosomes represent a versatile and promising research tool for studying sperm biology and provide new options for the diagnosis and treatment of male infertility.

Graphical abstract:



First draft submitted: 10 February 2020; Accepted for publication: 2 June 2020; Published online: 14 August 2020

Keywords: delivery tool • exosome • infertility • reproductive medicine • sperm

Advances in nanomedicine have led to the targeted delivery of diagnostic and therapeutic agents to single tissues or cell types, thereby fostering a noninvasive treatment that rivals the ability of engineered nanomaterials. Infertility is defined as the inability to conceive after 1 year of unprotected sexual intercourse and affects approximately 15% of couples worldwide [1]. According to the Human Fertilisation and Embryology Authority (HFEA), up to 50% of human infertility cases are male-related [2,3]. In many cases, male infertility has a genetic origin leading to critical abnormalities in sperm function [4–6]. Consequently, there is an urgent need to develop appropriate technologies with which to investigate, diagnose and treat, abnormal sperm. However, our ability to design such methodologies is restricted by the inherent resistance of sperm to the uptake of exogenous compounds [7,8]. Therefore, if we are to stand any chance of understanding and targeting the aberrant molecular mechanisms responsible for male infertility, it is vital that we develop a system capable of delivering biological agents into sperm without causing detrimental effects on basic sperm function, such as the ability to swim and undergo the capacitation process prior to oocyte fertilization.

Several approaches have been developed to treat sperm-borne abnormalities. Thus far, synthetic lipid and polymer-based carrier systems have been proven useful for reproductive purposes, successfully targeting mammalian sperm [9,10]. More specifically, these studies have demonstrated the ability of these nanocarriers to penetrate the inert envelope of sperm. Najafi and colleagues reported that the effects of an antioxidant in rooster sperm were enhanced when delivered by liposomes when compared with incubation with the agent alone, consequently proving that such delivery systems could introduce beneficial molecules that can enhance sperm functionality [10].

However, these artificial systems have raised several concerns relating to their non-biodegradability and immunogenic effects [11,12]; thus paving the way for the development of cell-friendly alternatives such as extracellular vesicles (EVs) [13]. There are many different types of these enclosed lipid-bilayer structures that serve as a powerful form of intercellular communication for proteins, nucleic acids and lipids [14,15]. EVs can also act as a therapeutic tool since they are capable of crossing tissue barriers [16] and have higher rates of cellular uptake than their synthetic counterparts [17]. The cargo and composition of the EVs is dependent on the mother cell type and physiological state. There have been identified specific membrane protein markers and intraluminal molecules for each classified EV subtype [14,15,18,19].

EVs are secreted by all human tissues, and have been isolated from several sources, including widely available cell lines, such as human embryonic kidney (HEK293T) cells, which for instance have been shown to lack cancer-related and immunogenic-induction mechanisms, thus representing a safe source of EVs to work with under *in vitro* and *in vivo* conditions [20–22]. These cell types also allow a scalable manufacturing system for the mass production of EVs, having been cultured inside specific bioreactors for this purpose [23]. Finally, EVs derived from HEK293T cells have also been demonstrated to exhibit significant versatility in terms of their cell targeting ability [24].

The present literature shows that EVs are currently being developed for a range of biomedical applications due to their potential for *in vivo* and *in vitro* delivery [24–28]. In particular, exosomes, the smallest form of EVs (size ranging from 30 to 200 nm) [29], are becoming very popular from a diagnostic and therapeutic point of view in a wide spectrum of cells, including induced pluripotent stem cells and tissues [24–34].

Several studies have incubated mammalian sperm with exosomes that were isolated from seminal fluid [35–39]; these exosomes are sometimes referred to as prostasomes [40]. A previous study reported that prostasomes were successfully able to transfer proteins into sperm [35]. However, there has been no attempt to investigate the safety and feasibility of deploying exosomes isolated from a commercially available cell line, with scalable options and manufacturing opportunities, as an efficient tool for the delivery of compounds into mammalian sperm. Moreover, it is important to consider that there are certain clinical scenarios where it is not possible to collect or use seminal fluid from male patients, such as cases involving testicular cancer or those suffering from obstructive or ejaculatory problems [41,42]. Therefore, there is an urgent need to evaluate whether cell line based exosomes can be used to deliver compounds to gametes in a safe manner; further research is urgently required.

In the present study, we aimed to develop an alternative mammalian-based manufacturing system with scalable applications, for the isolation and exploitation of exosomes as a noninvasive approach for mammalian sperm. We isolated exosomes from a commonly used cell line and describe the results of a number of experiments designed

to evaluate whether incubation with exosomes would cause deleterious effects on key aspects of sperm function. We chose boar sperm as an animal model due to its morphological and biological similarities with human sperm. We isolated and fluorescently labelled HEK293T-derived exosomes to investigate their potential for interaction with boar sperm during simple *in vitro* co-incubation. We also found that exposure to exosomes had no detrimental effect upon the functionality of boar sperm in terms of viability and ability to undergo *in vitro* capacitation. Our data show that exosomes derived from HEK293T spontaneously interact with boar sperm *in vitro* and provides proof-of-concept for the future exploitation of this tool in a noninvasive manner and may help us to develop novel options for the diagnosis and treatment of male infertility.

Materials & methods

Additional information is provided in the [Supplementary data](#).

Mass production of exosomes from HEK293T cells

A total of 500–600 ml of culture media from HEK293T cell culture were collected; this was centrifuged ($500\times g$ at 4°C for 10 min) and the resulting supernatant was filtered through a $0.20\text{-}\mu\text{m}$ filter. The filtrate was then centrifuged at $150,000\times g$ for 2 h at 4°C in a Beckman Coulter L-80 UC ultracentrifuge equipped with a SW 32 Ti Swinging-Bucket Rotor (Beckman Coulter, UK), as previously described [43].

Exosome labelling

Exosomes were fluorescently labelled with $2\text{ }\mu\text{g/ml}$ of wheat germ agglutinin WGA-AlexaFluor488 conjugate (Thermo Fisher Scientific, UK). A negative control, phosphate-buffered saline (PBS), was stained and washed in parallel.

Exosome characterisation

A number of techniques were carried out to prove that samples contained exosomes, including nanoparticle tracking analysis (NTA), the bicinchonic acid assay (BCA) for total protein quantification, western blotting and transmission electron microscopy (TEM). These techniques were carried out in strict accordance with the Minimal Information for Studies of Extracellular Vesicles 2018 (MISEV2018) guidelines to ensure that each sample was evaluated accurately with respect to sample purity and exosome integrity [19].

Nanoparticle tracking analysis

The concentration and size profiles of each exosome sample ($n = 3$) were determined with a NanoSight NS500 equipped with a 488 nm laser (Malvern, UK), by following a previously described protocol [44].

Protein quantification

The BCA protein assay kit (Pierce, Paisley, UK) was used to determine the total protein content in each exosome sample, each assay was performed in triplicate. Protein concentrations were extrapolated from a standard curve using a linear equation.

Western blotting

Western blotting was carried out by loading exosome samples in triplicate alongside their source material lysate (HEK293T cell lysate). Each sample contained an equivalent amount of total protein ($10\text{ }\mu\text{g}$) in order to compare different markers between the exosome samples and the cells from which they were derived. Membranes were incubated with primary antibodies against specific exosome markers (*ALIX*, *SYNTENIN-1* and *CD9*). As negative controls, membranes were also incubated with primary antibodies against other cellular compartments (*CALNEXIN*, *CYTOCHROME-C* and *LAMIN A*). Further details relating to these protein markers are given in [Supplementary Table 1](#). Specific details for the primary and secondary antibodies are detailed in [Supplementary Table 2](#). The relative amount of protein in each lane was normalised against the band intensities obtained in cell lysates.

Transmission electron microscopy

High-resolution TEM images were acquired with a FEI Tecnai 12 microscope operating at 120 kV, and equipped with a Gata OneView camera (Electron Microscopy Facility, Dunn School of Pathology, University of Oxford).

Preparation & in vitro incubation of sperm samples

All boar semen samples were obtained from two suppliers (Servicios Genéticos Porcinos; Masies de Roda, Barcelona, Spain and JSR Genetics, Cambridge, UK). A total of ten ejaculates from ten different boars were collected, and for each replicate two different seminal doses were pooled together ($n = 5$) in order to reduce the effect of interindividual variation. The capacitating buffer used for the *in vitro* incubation of sperm samples was prepared fresh with 20 mM 4-(2-hydroxyethyl)-1-piperazineethanesulfonic acid (HEPES), 112 mM NaCl, 3.1 mM KCl, 5 mM glucose, 21.7 mM L-lactate, 1 mM sodium pyruvate, 0.3 mM Na_2HPO_4 , 0.4 mM MgSO_4 , 4.5 mM CaCl₂, 19 mM of NaHCO_3 and 5 mg/ml of bovine serum albumin (pH = 7.4) as described previously but with some modifications [45]. Further *in vitro* capacitation was enhanced by triggering acrosome exocytosis with the addition of progesterone (10 $\mu\text{g}/\text{ml}$), as previously described [46,47].

Evaluation of exosome–sperm interaction by total internal reflection fluorescent microscopy

The evaluation of exosome interaction with sperm was performed using five different boar ejaculates ($n = 5$). Each semen sample was split into two aliquots: one for exosome-treatment and one as to act as control. The exosome-treatment aliquot was mixed with WGA-labelled exosomes to a final concentration of 10^8 EV/ml; this created an exosome to sperm working ratio of 100:1 in capacitating buffer. Incubation was carried out for 5 h and progesterone was added 4 h post incubation. Aliquots from exosome-treated and control samples were evaluated at 10 min and 2 h after incubation began, and at 30 and 60 min after the addition of progesterone (4 h 30 min, and 5 h after incubation began, respectively).

For total internal reflection fluorescent microscopy (TIRFM) imaging, treated and control sperm samples were fixed with 10% formalin. After fixation, sperm was labelled for 10 min with 10 $\mu\text{g}/\text{ml}$ of WGA-AlexaFluor647 conjugate to visualise the exosomes and sperm membrane. This protocol allowed us to distinguish exosomes that had been internalized by the sperm, as it relies on the fact that the WGA-AlexaFluor488 label will stain the previously labelled exosomes with WGA-AlexaFluor647, by filling up the gaps in the exosome's surface, but only those that have not been internalized inside the sperm, thus exhibiting both red and green fluorescence. All of the sperm cells undergoing imaging exhibited at least one exosome, either bound or internalized.

Effects of exosome–sperm interaction during *in vitro* capacitation & progesterone-induced acrosome reaction

Semen samples were split into four aliquots: one served as a control, whereas the other three were for different exosome treatments: 10^7 , 10^8 and 10^9 EV/ml (exosome to sperm working ratios of 1:1, 10:1 and 100:1, respectively). Incubation was carried out for 5 h and progesterone was added 4 h after incubation began. At 10 min, 2 h and 4 h after incubation began and at 10, 30 and 60 min after the addition of progesterone (4 h 10 min, 4 h 30 min and 5 h after incubation began, respectively), we evaluated sperm motility, viability, membrane lipid disorder and mitochondrial membrane potential.

Analysis of sperm motility

Sperm motility was assessed using a Hamilton Thorne Computer Assisted Sperm Analyser (CASA) system (software version 12.3; Hamilton-Thorne Research, USA) using a Nikon Eclipse 80i microscope (Nikon, Japan). This system allowed us to objectively classify individual sperm according to different kinematic parameters that were measured from digital images extracted from recorded sperm tracks [48]. For this study, we considered the parameters assessed by the system that are descriptive of the sperm sample's motion and trajectory; total motility (%), progressive motility (%), smooth path velocity (VAP, $\mu\text{m}/\text{s}$), straight line velocity (VSL, $\mu\text{m}/\text{s}$), track velocity (VCL, $\mu\text{m}/\text{s}$), straightness (STR: VSL/VAP , %), linearity (LIN: VSL/VCL , %) and wobble (WOB: VAP/VCL , %).

Flow cytometry analysis

Sperm viability, membrane lipid disorder or membrane fluidity (MF) and mitochondrial membrane potential (MMP) were determined by a Cell Laboratory QuantaSC™ cytometer (Beckman Coulter; CA, USA; Serial Number: AL300087) using single-line visible light (488 nm) from an argon laser.

Sperm viability was assessed using a SYBR-14/propidium iodide (PI) assay according to the protocol described by Garner and Johnson (1995) [49]. Sperm that were positive for SYBR-14 and negative for PI (SYBR-14⁺/PI[−]) were classified as viable. MF was evaluated by co-staining with Merocyanine 540 (M-540) and YO-PRO®-1 as described by Harrison *et al.* (1996) [50]. Sperm that were negative for M-540 and YO-PRO (M-540[−]/YO-PRO[−])

were viable and had low levels of membrane lipid disorder. MMP was analysed by incubation with JC-1 [51]. Two emission filters (FL-1 and FL-2) were used to detect and differentiate two sperm populations; JC-1 aggregates (JC-1_{agg}) and JC-1 monomers. Sperm from the JC-1_{agg} population were classified as presenting with high MMP.

Statistical analysis

Results from CASA and flow cytometry were analysed using the SPSS statistical package for Windows (Ver. 25.0; NY, USA). Data were first evaluated for normality (Shapiro-Wilk test) and homogeneity of variances (Levene test). Following this, we applied a mixed model (between-subjects factor: treatment; within-subjects factor: incubation time) followed by a *post-hoc* Sidak test for pair-wise comparisons. Each sperm parameter was considered as an independent variable. The level of significance was set at $p \leq 0.05$, and data are shown as mean \pm standard error of the mean (SEM).

Results

Production, characterization & quality assessment of HEK293-derived exosomes

NTA, BCA, western blotting and TEM were used to quantify and determine the quality and efficiency of the isolation protocols designed for the synthesis and enrichment of HEK293T-derived exosomes.

Nanoparticle tracking analysis

Size profiles for the samples of HEK293-derived exosomes were obtained by NTA and are shown in Figure 1A. In all three profiles, the larger peaks showed a mean modal size of 167.1 nm (153.7 ± 6.6 nm, 171 ± 6.0 nm; and 176.7 ± 8.1 nm), and an average percentage of 72.3 of particles with a size <200 nm. Additional smaller peaks, representing larger particle sizes, were also apparent, and are most likely to correspond to aggregates of exosomes. The total mean concentration represented by the area under all three curves is 1.23×10^{10} EV/ml.

Degree of purity

Protein assays showed a mean total protein concentration of 0.26 mg/ml. These results, together with the total concentration of exosomes obtained by NTA were used to determine the degree of purity of the exosome samples, as described by Webber and Clayton [52]. These authors concluded that ratios $>3 \times 10^{10}$ EV/mg equate to high vesicular purity, ratios of 2×10^{10} to 2×10^9 EV/mg represent low purity, and any ratios below 1.5×10^9 EV/mg represent not pure. The EV:protein ratio for our exosome samples was determined to be 4.73×10^{10} EV/mg (1.23×10^{10} EV/ml), indicating that our samples had high vesicular purity.

Transmission electron microscopy

TEM revealed membranous vesicles present in the exosome samples. Further analysis, using Image J software, indicated that these structures were approximately 40 nm in diameter (Figure 1B).

Western blotting

Western blotting was performed with 10 μ g of total protein and used to determine the relative expression levels of protein markers in our exosome samples. The mean density of each band was quantified from chemiluminiscent blots using the GeneTools software.

The negative control markers (CALNEXIN, LAMIN-A and CYTOCHROME C) were expressed in the HEK293T cell lysates. However, no bands for CYTOCHROME-C and LAMIN A were present in the exosome lysates (Figure 1C). While CALNEXIN was present in both HEK293T cell lysates and exosome lysates, the mean band density corresponding to this protein was 0.36 times higher in cell lysates than in the exosome lysates.

Specific-exosomal protein markers (*ALIX*, SYNTENIN-1 and CD9) were expressed in all exosome samples (Figure 1D); lane 1 shows that there were no bands in the HEK293T cell lysate for either *ALIX* or SYNTENIN-1. There was a weak band for CD9 in the HEK293T cell lysate (lane 1); the mean band density for this protein marker in exosome lysates (lanes 2, 3 and 4) was 0.20-times higher than in the HEK293T cell lysate.

Experiment 1: evaluation of exosome–sperm interaction by TIRFM

The efficiency of exosome–sperm interaction, including the binding and internalization of exosomes within individual sperm was determined qualitatively by TIRFM.

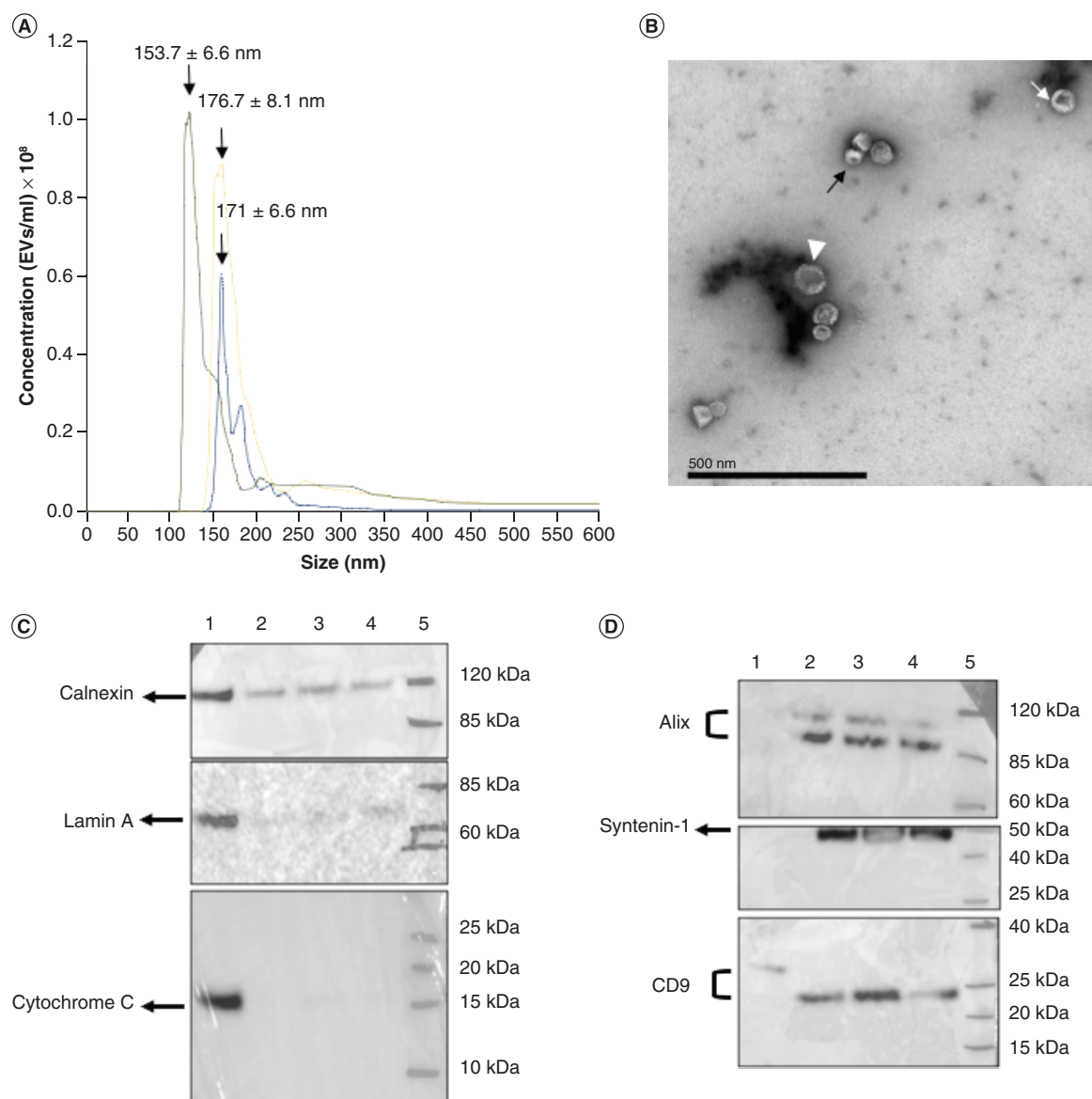


Figure 1. Characterization of exosome-enriched samples derived from HEK293T cells. (A) Size and concentration profile, as analysed by nanoparticle tracking analysis, showing three peaks with a modal size of 153.7 \pm 6.6 nm, 176.7 \pm 8.1 nm and 171 \pm 6.6 nm (n = 3). (B) Image taken by transmission electron microscopy (120 kV) showing exosome-like vesicles of ~50 nm diameter (white arrow head), exosome-like vesicles of ~40 nm diameter (white arrow) and exosome-like vesicles with a diameter of ~30 nm (black arrows). Scale bar: 500 nm. (C & D) Show western blotting images of the protein expression levels for negative control markers (CALNEXIN, LAMIN-A and CYTOCHROME-C) at ~90, ~69 and ~12 kDa, respectively, and the exosomal markers (ALIX, SYNTENIN-1 and CD9) at ~97, ~35 and ~25 kDa, respectively. Lane 1 corresponds to HEK293T cell lysates, lane 2–4 correspond to exosome samples (n = 3) and lane 5 corresponds to the protein marker. The density of protein bands was identified and manually selected for quantification on chemiluminescent blots using GBOX Chemi XX6/XX9 equipped with GeneTools software, by normalizing the relative protein amount in each lane against the band intensities obtained from HEK293 T cell lysates. Strong bands can be seen for CYTOCHROME-C and LAMIN-A in HEK293T cell lysate (lane 1), while no bands are present in the exosome samples shown in lanes 2, 3 and 4. CALNEXIN expression can be seen as fainter bands in the exosome lysates (lanes 2, 3 and 4) with a mean band density that is 0.36-times lower when compared with the HEK293T cell lysate (lane 1). With regard to the exosomal markers, no bands are visible for ALIX and SYNTENIN-1 in the HEK293T cell lysates shown in lane 1, and stronger bands can be seen for exosome lysates (lanes 2, 3 and 4). CD9 was clearly evident in lane 1; the mean band density for this protein marker in the exosome lysates (lanes 2, 3 and 4) was 0.20-times higher than in the HEK293T cell lysates.

Images acquired by TIRFM showed the HEK293-derived exosomes as green fluorescent particles that were either associated or internalized inside the sperm portions, being observed such an association being more localised in the sperm tail and mid-piece at 10 min, 2 h, 4 h, 30 min and 5 h post incubation (Figure 2A). Exosomes associated with sperm exhibited both green and red WGA labelling giving a slightly orange signal (yellow arrow heads), while exosomes that had been internalized only exhibited green WGA labelling (white arrow heads). The untreated control at 5 h post incubation showed no presence of green WGA-AlexaFluor488 dye. At 10 min post incubation both surface bound and internalized exosomes in orange and green fluorescence, respectively, can be seen.

During analysis, we paid particular attention to exosome internalization. Figure 2B and C shows two TIRFM images presenting two distinct sperm cells at 5 h post incubation; the exosomes are shown within the white squares. Figure 2B is a high resolution image and shows attached exosomes as an orange-like color; this is due to the combination of the red and green signals in the composite channel that can also be seen individually in the WGA-AlexaFluor647 (white arrows) and WGA-AlexaFluor488 channels, respectively. Similarly, Figure 2C shows a close-up of a signal display for internalized exosomes; here, only the green dye is evident, both in the composite and WGA-AlexaFluor488 channels.

Experiment 2: effects of exosome–sperm interaction during *in vitro* capacitation & progesterone-induced acrosome reaction

Boar sperm were exposed to exosomes and co-incubated *in vitro* under capacitating conditions. Exogenous progesterone was added 4 h post incubation in order to mimic the environment experienced by sperm in the female reproductive tract. We then tested a range of key functional parameters, including motility, viability, MF and MMP to indicate whether exposure to exosomes had any deleterious effects on the sperm.

With regard to sperm motility, none of the exosome treatments had any significant effects upon total sperm motility when compared with the control. However, a slight, but not significant, increase in sperm motility was observed for the 1:1 exosome treatment; this was the case at all time points except at 4 h 30 min post incubation (Figure 3A). This effect was even more pronounced with the 1:1 treatment for progressive motility, which was significantly higher when compared with the 100:1 treatment ($p < 0.01$) at 10 min post incubation (Figure 3B). At this particular time point, the progressive motility in the 100:1 treatment was also significantly lower than that of the control ($p < 0.05$).

As far as the other kinematic parameters are concerned, no significant differences were observed between the controls and the exosome treatments at any given time point (Supplementary Table 3), except for LIN and WOB. Our analysis showed that in the 100:1 exosome treatment, LIN was significantly ($p < 0.05$) lower than in the 1:1 treatment after 4 h 30 min of incubation (Figure 3C). After 4 h 10 min of incubation, WOB was significantly higher in the 100:1 exosome treatment than in the rest of the treatments including the control ($p < 0.01$ when compared with the control; $p < 0.01$ when compared with the 1:1 treatment; and $p < 0.05$ when compared with 10:1). WOB was inversely proportional to the concentration of exosomes at 4 h 10 min (Figure 3D). On the other hand, we observed a decreasing trend for all treatments, and the control, for most sperm kinematic parameters as the period of incubation progressed. However, LIN was seen to increase after 4 h 10 min of incubation, in both the control, and all treatments; this increase was more pronounced at the 1:1 ratio (Figure 3C).

With regard to sperm viability, membrane lipid disorder and mitochondrial membrane potential, we observed no significant differences between the control and treatments (100:1, 10:1 and 1:1) at any of the tested time points (Table 1–Table 3). As expected, there was a reduction in the proportion (%) of viable spermatozoa (SYBR-14⁺/PI⁻), viable spermatozoa with low membrane lipid disorder (M540⁻/YO-PRO-1⁻) and viable spermatozoa exhibiting high mitochondrial potential (JC-1_{agg}), in the controls and treatments, as the incubation time progressed. Supplementary Figures 1–3 show these different sperm populations analysed by flow cytometry after 10 min and 4 h 10 min as examples of short-term incubation and long-term incubation, respectively, following the addition of progesterone.

Discussion

Exosomes have been widely used as an *in vivo* and *in vitro* vehicle for biological compounds by virtue of their natural properties, in comparison to other forms of delivery systems. However, their application as a nanotool is only just beginning in the field of reproductive medicine, and further research is required to explore the feasibility, reproducibility and safety issues of this approach before being able to consider this methodology for future clinical purposes.

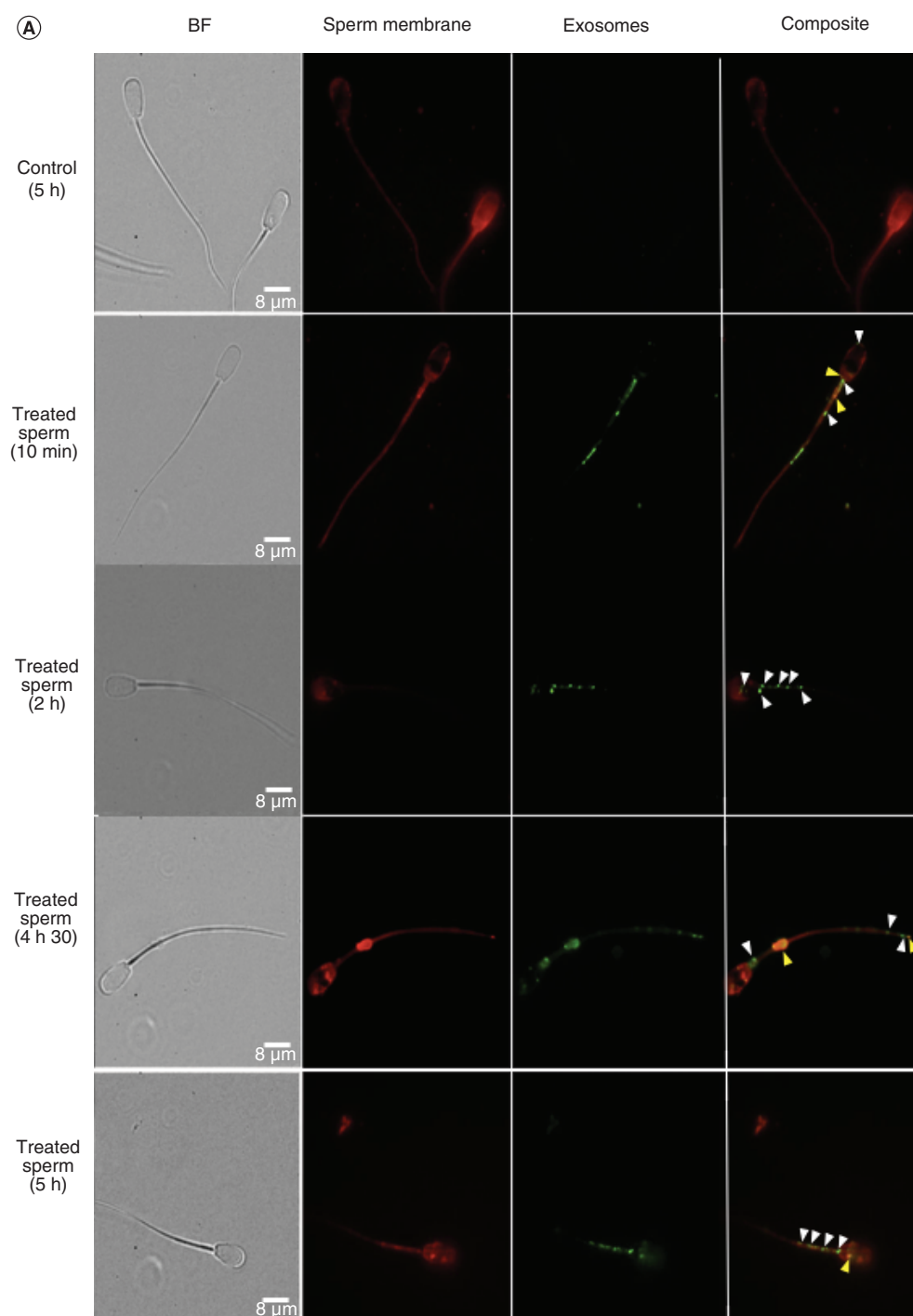


Figure 2. Visualization of exosome–sperm interaction after *in vitro* co-incubation of boar sperm with 100:1 HEK293-derived exosome treatment using total internal reflection fluorescence microscope. Total internal reflection fluorescence microscope images of exosome samples (WGA-AlexaFluor488, green) that were incubated with sperm samples for the indicated times. After fixation, sperm were labeled with wheat germ agglutinin (WGA-AlexaFluor647, red) to visualise the sperm membrane. **(A)** The presence of an intact sperm is indicated by the bright field image (BF). Images show different sperm cells. Control sperm samples at 5 h post incubation and exosome treated samples at 10 min, 2 h, 4 h 30 min and 5 h post incubation. White arrow heads indicate internalized exosomes within the sperm cells, yellow arrow heads indicate attached exosomes outside the sperm cells. Scale bar = 8 μ m. **(B & C)** Total internal reflection fluorescence microscope images show two different sperm cells treated with exosomes after 5 h incubation. Regions delineated by white squares have been magnified ($z = 0, 500\text{-}$ and 1000- times) to show signal displays in the composite, WGA-AlexaFluor647 (red) and WGA-AlexaFluor488 (green) channels. **(B)** shows a sperm representative to those sperm with an attached exosome; note the green and red signals that are evident in the red (white arrows) and green channels, respectively. **(C)** shows a sperm representative to those sperm with internalized exosomes, as it is visible from only a green signal display in the green and composite channels. Scale bars are 5 and 2 μ m. BF: Bright field.

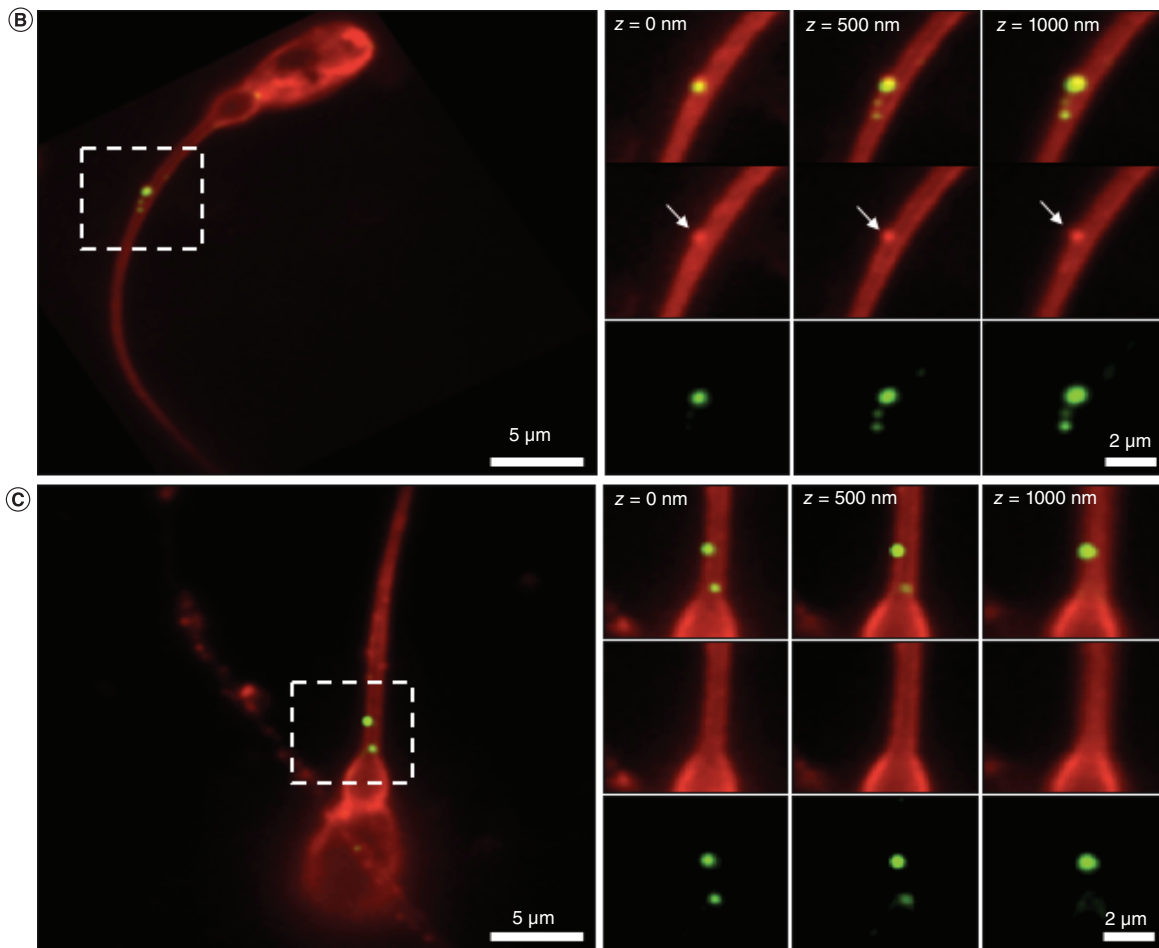


Figure 2. Visualization of exosome-sperm interaction after *in vitro* co-incubation of boar sperm with 100:1 HEK293-derived exosome treatment using total internal reflection fluorescence microscope (cont.). Total internal reflection fluorescence microscope images of exosome samples (WGA-AlexaFluor488, green) that were incubated with sperm samples for the indicated times. After fixation, sperm were labeled with wheat germ agglutinin (WGA-AlexaFluor647, red) to visualise the sperm membrane. **(A)** The presence of an intact sperm is indicated by the bright field image (BF). Images show different sperm cells. Control sperm samples at 5 h post incubation and exosome treated samples at 10 min, 2 h, 4 h 30 min and 5 h post incubation. White arrow heads indicate internalized exosomes within the sperm cells, yellow arrow heads indicate attached exosomes outside the sperm cells. Scale bar = 8 μ m. **(B & C)** Total internal reflection fluorescence microscope images show two different sperm cells treated with exosomes after 5 h incubation. Regions delineated by white squares have been magnified ($z = 0, 500$ - and 1000 -times) to show signal displays in the composite, WGA-AlexaFluor647 (red) and WGA-AlexaFluor488 (green) channels. **(B)** shows a sperm representative to those sperm with an attached exosome; note the green and red signals that are evident in the red (white arrows) and green channels, respectively. **(C)** shows a sperm representative to those sperm with internalized exosomes, as it is visible from only a green signal display in the green and composite channels. Scale bars are 5 and 2 μ m. BF: Bright field.

The present work evaluates human-derived exosomes for their future potential as a noninvasive delivery system for mammalian sperm. We demonstrate that exosomes derived from HEK293 T cells can be used *in vitro* with mammalian sperm without causing detrimental effects on sperm structure or function and may be developed further to deliver selective compounds. The rationale behind isolating exosomes from HEK293T cells relies upon their proven capability for the mass production of exosomes, thus allowing the manufacturing process to be scaled-up for future industrial and clinical applications.

At the present time, there is no specific consensus regarding the size range, morphology, or exosomal markers. This is because these parameters depend on the source and biogenesis pathway from which they originate and also because different theories have been put forward to explain the biogenesis of exosomes; these theories differ with

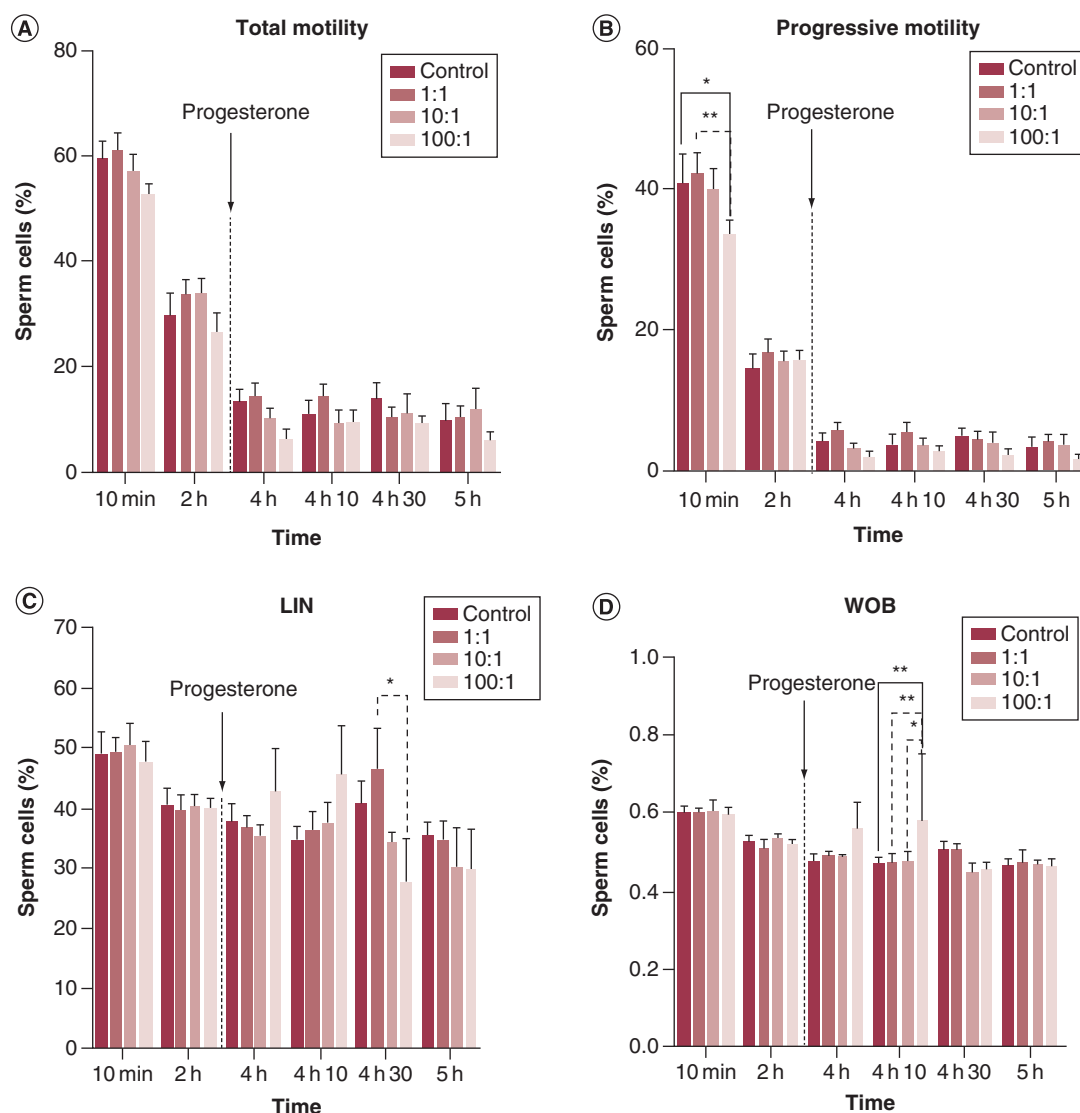


Figure 3. Motility parameters of boar sperm, as determined by computer assisted sperm analysis after *in vitro* co-incubation with different HEK293-derived exosome treatments (1:1, 10:1, and 100:1 exosome to sperm ratios) compared with controls. Data are shown as (means \pm scanning electron microscopy from 5 replicates in the control and treatment groups, $n = 5$). Progesterone was added at 4 h post incubation. **(A)** Total motility declines over time in all the treatments including the control with no significant differences between them ($p > 0.05$). **(B)** Progressive motility is significantly lower for the 100:1 treatment when compared with the time-matched control and 1:1 treatment ($p < 0.05$ and $p < 0.01$, respectively) at 10 min post incubation. **(C)** Linearity was significantly lower for the 100:1 treatment when compared with the time-matched 1:1 treatment at 4 h 30 min post-incubation ($p < 0.05$) and finally wobble. **(D)** was significantly increased for the 100:1 treatment when compared with the time-matched control, 1:1 and 10:1 treatments at 4 h 10 min post incubation ($p < 0.01$; $p < 0.01$ and $p < 0.05$, respectively). * $p < 0.05$; ** $p < 0.01$.

regard to the specific molecular machinery involved [14,15,18,19]. Moreover, several previous studies have shown that exosomes are associated with high levels of morphological heterogeneity [53,54]. Despite this variability, most authors recognize exosomes as small rounded vesicles with a membrane of 30–200 nm in size [19]. In accordance with this size range, and by using existing isolation techniques, it is impossible to solely isolate or purify one single subtype of EV, as they share common physical and biological properties [55]. Nonetheless, quality validations of our HEK293-derived exosome samples carried out using standardized techniques for exosome detection, revealed high concentrations of functional exosomes of high purity and with homogeneous morphology and size. It is worth mentioning that the size difference in the exosomes by TEM compared with NTA (~40 and ~170 nm,

Table 1. Descriptive data for the population of viable sperm (SYBR-14⁺/PI⁻) by flow cytometry for the different treatments (control, 1:1, 10:1 and 100:1 exosomes to sperm cell ratios) at different incubation times (n = 5).

Incubation time	Viable sperm (SYBR-14 ⁺ /PI ⁻)			
	Control	1:1	10:1	100:1
	Mean ± SEM* (%)	Mean ± SEM* (%)	Mean ± SEM* (%)	Mean ± SEM* (%)
10 min	55.61 ± 6.32	54.32 ± 6.65	52.58 ± 5.79	41.70 ± 10.59
2 h	29.19 ± 9.40	13.03 ± 5.71	25.71 ± 3.41	19.67 ± 4.77
4 h	23.08 ± 3.67	22.42 ± 1.79	24.41 ± 4.06	25.93 ± 3.51
4 h 10 min	13.28 ± 2.80	10.97 ± 2.94	17.40 ± 3.94	14.73 ± 6.36
4 h 30 min	15.98 ± 2.35	14.84 ± 3.23	13.18 ± 2.73	13.18 ± 2.95
5 h	14.81 ± 3.11	13.90 ± 1.45	20.34 ± 1.68	16.44 ± 2.04

Table 2. Descriptive data for the population of viable sperm with low membrane fluidity (M-540⁻/YO-PRO⁻) by flow cytometry for the different treatments (control, 1:1, 10:1 and 100:1 exosomes to sperm cell ratios) at different incubation times (n = 5).

Incubation time	Viable sperm with low membrane fluidity (M-540 ⁻ /YO-PRO ⁻)			
	Control	1:1	10:1	100:1
	Mean ± SEM* (%)	Mean ± SEM* (%)	Mean ± SEM* (%)	Mean ± SEM* (%)
10 min	58.18 ± 10.77	57.17 ± 11.03	60.19 ± 10.61	57.39 ± 10.10
2 h	33.30 ± 5.78	29.93 ± 6.58	27.30 ± 6.20	30.12 ± 5.15
4 h	19.19 ± 2.70	18.79 ± 3.08	17.68 ± 4.36	16.08 ± 2.69
4 h 10 min	15.41 ± 4.10	13.82 ± 4.75	16.61 ± 1.94	12.90 ± 4.18
4 h 30 min	26.78 ± 14.40	29.55 ± 14.80	28.53 ± 14.85	28.70 ± 14.60
5 h	24.88 ± 12.70	30.93 ± 11.34	25.53 ± 13.28	25.06 ± 12.93

Table 3. Descriptive data for the population of sperm exhibiting high mitochondrial membrane potential (JC-1_{agg}) by flow cytometry for the different treatments (control, 1:1, 10:1 and 100:1 exosomes to sperm cell ratios) at different incubation times (n = 5).

Incubation time	Viable sperm exhibiting high mitochondrial membrane potential (JC-1 _{agg})			
	Control	1:1	10:1	100:1
	Mean ± SEM* (%)	Mean ± SEM* (%)	Mean ± SEM* (%)	Mean ± SEM* (%)
10 min	65.46 ± 6.86	63.55 ± 5.29	55.19 ± 10.42	61.95 ± 6.16
2 h	50.16 ± 1.25	53.25 ± 1.80	51.85 ± 5.29	47.49 ± 7.27
4 h	44.80 ± 8.46	42.82 ± 7.40	45.13 ± 9.76	43.31 ± 7.91
4 h 10	34.15 ± 4.67	41.06 ± 14.21	38.16 ± 9.85	39.56 ± 12.4
4 h 30	43.65 ± 17.50	55.17 ± 13.18	42.89 ± 14.41	31.68 ± 8.53
5 h	31.85 ± 6.24	26.01 ± 7.09	33.33 ± 5.55	32.15 ± 5.03

respectively) may be due to the fact that NTA can only detect particles above 70 nm [44], and also, may be due to a possible exosome shrinkage previously reported as an artifact from TEM processing [14]. Furthermore, the absence or reduced quantities of other cellular compartments (endoplasmic reticulum, nucleus and mitochondria), in the samples used for Western blotting eliminates the possibility that larger EV subtypes such as oncosomes could be present and confirm the presence of exosomes only.

Our experiments clearly demonstrated exosome–sperm interaction when boar sperm was co-incubated *in vitro* with human WGA-labelled exosomes at a 100:1 exosome to sperm ratio at 10 min, 2 h, 4 h 30 min and 5 h post incubation. Exosome binding and internalization was observed after only 10 min of incubation, suggesting that exosome–sperm interaction is a rapid process, as previously highlighted in another study [37]. Interestingly, we demonstrate that interaction takes place preferentially in the sperm's tail and mid-piece over the sperm's head, yet exosome internalization was observed within 10 min of incubation, thus confirming that this interaction was efficient and did not only take place on the outer surface of the sperm.

It is worth noting that our experiments were carried out under capacitating conditions, with a pH of 7.4, in order to trigger the sequence of structural and metabolic changes that the sperm must undergo in order to be able to fertilise the oocyte. Some studies have shown that prostasome fusion with sperm cells can only take place in an acidic environment, rather than at neutral pH or a slightly alkaline one [56,57].

As for the mechanisms governing exosome uptake, several studies support the fact that exosomes can undergo endocytosis and that this may be the dominant method of EV uptake [58]. However, sperm cells lack endocytic pathways; instead, there is some evidence for membrane fusion as the preferred mechanism of interaction between prostasomes and sperm [40]. Nonetheless, there is a significant lack of understanding with regard to this interaction. Indeed, a previous study, which described the use of prostasomes to transfer proteins into boar sperm, proposed that the cytoskeleton might be involved in the uptake mechanism [35]. Further studies may elucidate the molecular pathways by which HEK293-derived exosomes interact with sperm.

In addition, our study revealed that the incubation of boar sperm with exosomes at a ratio of 100:1 led to a significant reduction in progressive motility after just 10 min of incubation. This effect was even more apparent when compared with the lowest exosome:sperm ratio (1:1) at this time point, which appeared to have a positive effect upon progressive motility compared with the untreated control. This effect may not be taken as deleterious, since the progressive motility was observed to be back to normal throughout the rest of the incubation period, and rather indicates to be in line with the observations made on the ability of HEK293-derived exosomes to spontaneously interact with sperm after only 10 min of co-incubation. Moreover, as expected, LIN, which should increase in response to capacitation, did show an increasing trend in all treatments, particularly after the addition of progesterone [59]. Nonetheless, LIN was significantly lower in the 100:1 than in the 1:1 treatment when tested 30 min of the addition of progesterone, thereby suggesting that such a high exosome concentration may be interfering with the sperm ability to undergo capacitation. However, it is also worth discussing that in this same treatment (100:1), WOB was significantly higher than the control and other treatments; in fact, the pattern at 4 h 10 min followed a proportional correlation to the concentration of exosomes. While no previous studies have correlated WOB with capacitation, an increase in WOB, showing a smoother and more curvilinear motion, has been previously described for fresh human and boar sperm samples in response to capacitating conditions [47,60]. Coupled with these studies, our present data suggest that sperm with the highest exosome treatment (100:1) achieved a higher capacitation status 10 min after the addition of progesterone than the control or other treatments.

In the last part of our study, we investigated sperm viability, membrane lipid disorder and mitochondrial membrane potential in order to gain a more reliable prediction of the ability of sperm to undergo capacitation when subjected to exosome treatment. Remarkably, the exposure of boar sperm to HEK293-derived exosomes had no effect upon these three parameters, at least when evaluated by flow cytometry; this effect was evident when comparisons were made between the control and treatments for all the three sperm: exosome ratios. Consequently, despite the effects observed in some of the sperm motility parameters for the lowest and highest treatments (1:1 and 100:1, respectively), co-incubation of high concentrations of HEK293-derived exosomes with boar sperm did not interfere with their ability to undergo the functional changes that occur during capacitation. These results differ from previous studies, which found that cholesterol from prostasomes was transferred to the sperm membrane, thereby decreasing their lipid disorder, and thus the membrane's fluidity during the process of capacitation [61,62], resulting in a reduction of the proportion of capacitated sperm [63]. In addition, others have found that prostasomes stimulate the acrosome reaction when they fuse with sperm, thus rendering them to be more sensitive to progesterone [64–66]. In our study, however, there was no evidence for such an impact when using HEK293-derived exosomes. These discrepancies may be related to the biological differences between HEK293-derived exosomes and prostatic EVs, which have been shown to be more sperm-specific. That being said, this effect could also be explained by the fact that other seminal components could inevitably be carried, together with EVs, by sperm, as other studies have reported that such changes take place when adding seminal plasma to frozen-thawed boar sperm [67,68]. In any case, further studies should address to which extent the particular nature of EVs, whether derived from epithelial cell lines, such as HEK293T, or from the male reproductive tract, has a specific impact upon the ability of sperm to capacitate and undergo acrosome exocytosis. Furthermore, our data warrant further research on the effects upon sperm capacitation that are closely related with sperm motility, such as the phosphorylation of tyrosine residues in sperm tail proteins, and the capacity of treated sperm to fertilise an oocyte *in vitro*. This would help to address the differences observed between sperm motility and the other sperm parameters.

In addition, although some studies have successfully used HEK293-derived exosomes *in vitro* and *in vivo* on a variety of different tissues from several animal species [25,27,28], it is worth considering whether the application of

exosomes may evoke an immune response when applied to boar sperm *in vivo*. Consequently, we must remember that the boar model is not entirely representative of the human, particularly with regard to the physiological response.

Conclusion

In conclusion, the current study describes, for the first time, an assessment of the cytotoxicity and potential for HEK293-derived exosomes to be applied *in vitro* as an efficient and noninvasive tool for mammalian sperm. Thus, our results serve as a proof-of-concept for the use of HEK293T cells as a mammalian-based system with scalable and commercial capabilities for exosome production. Hence, the further development of this approach toward its future application as either a diagnostic or therapeutic system for mammalian gametes, may offer a wider range of opportunities for infertile patients with compromised clinical scenarios, for instance by delivering protective agents and/or essential molecules capable of enhancing or restoring normal functionality to a damaged gamete.

Future perspective

With the increasing trend for infertility to cause serious impact on global birth rates, both developed and non developed countries have declared this condition of national interest and established policies that encourage research and development for new treatments. Male-related infertility problems account for up to 50% of infertility cases; in many of these cases, we have only limited, or no options, for successful diagnosis or treatment. We believe that the development of exosome-based delivery systems may provide us with a highly useful tool to develop new ways of studying sperm biology and allow us new options for the diagnosis and treatment of male fertility.

Summary points

- This study for the first time, utilized a mammalian-based manufacturing system based on a commercial cell line that allows the large-scale isolation of exosomes for their application in reproductive biology.
- In this study, we show for the first time the effects of *in vitro* short-term and long-term exposure of exosomes previously isolated from a human cell line for their use with mammalian sperm under conditions that mimic the fertilization scenario *in vitro*.
- This is the first time that super resolution microscopy techniques have been used to observe exosome interaction, to the single level, with mammalian sperm.
- The results from this study have revealed that HEK293T cell-derived exosomes interact with boar sperm and get internalized inside the sperm portions with 10 min of simple *in vitro* co-incubation.
- Computer Assisted Sperm Analysis has shown that 5-h *in vitro* exposure of HEK293T cell-derived exosomes does not significantly impact boar sperm's motility.
- Flow cytometry assays have revealed that 5-h *in vitro* exposure of HEK293T cell-derived exosomes does not significantly impact boar sperm's viability, membrane fluidity nor mitochondrial membrane potential.
- The present study shows that HEK293T cell-derived exosomes did not cause deleterious effect on any of the key sperm parameters studied; collectively, these factors are informative of the ability of sperm to undergo *in vitro* capacitation.
- This study can serve as a proof-of concept for the future development of exosomes as a novel therapeutic tool to deliver proteins and other molecules that may enhance the functionality of sperm.

Supplementary data

To view the supplementary data that accompany this paper please visit the journal website at: www.futuremedicine.com/doi/suppl/10.2217/nnm-2020-0056

Financial & competing interests disclosure

The authors acknowledge generous support from the Ministry of Science, Innovation and universities, Spain (grants: RYC-2014-15581 and AGL2016-81890-REDT), and the Regional Government of Catalonia, Spain (grant: 2017-SGR-1229), the Nuffield Department of Women's and Reproductive Health, University of Oxford, UK, the Wellcome Trust (100262Z/12/Z), Kennedy Trust for Rheumatology Research for Imaging facilities, and European Commission (ERC-2014-AdG_670930). The authors have no other relevant affiliations or financial involvement with any organization or entity with a financial interest in or financial conflict with the subject matter or materials discussed in the manuscript apart from those disclosed.

No writing assistance was utilized in the production of this manuscript.

Ethical conduct of research

The authors state that they have obtained appropriate institutional review board approval or have followed the principles outlined in the Declaration of Helsinki for all human or animal experimental investigations.

Open access

This work is licensed under the Creative Commons Attribution 4.0 License. To view a copy of this license, visit <http://creativecommons.org/licenses/by/4.0/>

References

Papers of special note have been highlighted as: • of interest; •• of considerable interest

1. Ombelet W, Cooke I, Dyer S, Serour G, Devroey P. Infertility and the provision of infertility medical services in developing countries. *Hum. Reprod. Update.* 14(6), 605–621 (2008).
2. Agarwal A, Mulgund A, Hamada A, Chyatte MR. A unique view on male infertility around the globe. *Reprod. Biol. Endocrinol.* 13, 37 (2015).
- **An overview of the prevalence of male infertility across the world, comparing developed and nondeveloped societies.**
3. Winters BR, Walsh TJ. The epidemiology of male infertility. *Urol. Clin. N. Am.* 41(1), 195–204 (2014).
4. de Kretser DM. Endocrinology of male infertility. *Br. Med. Bull.* 35(2), 187–192 (1979).
5. Kovac JR, Lamb DJ. Male infertility biomarkers and genomic aberrations in azoospermia. *Fertil. Steril.* 101(5), 31 (2014).
6. Amdani SN, Yeste M, Jones C, Coward K. Phospholipase C zeta (PLCzeta) and male infertility: Clinical update and topical developments. *Adv. Biol. Regul.* 61, 58–67 (2016).
7. Lenzi A, Gandini L, Picardo M, Tramer E, Sandri G, Panfilì E. Lipoperoxidation damage of spermatozoa polyunsaturated fatty acids (PUFA): scavenger mechanisms and possible scavenger therapies. *Front. Biosci.* 5, 1–15 (2000).
8. Tapia JA, Macías-García B, Miro-Moran A, Ortega-Ferrusola C, Salido GM, Peña FJ, Aparicio IM. The membrane of the mammalian spermatozoa: much more than an inert envelope. *Reprod. Domest. Anim.* 47(3), 65–75 (2012).
9. Barkalina N, Jones C, Townley H, Coward K. Functionalization of mesoporous silica nanoparticles with a cell-penetrating peptide to target mammalian sperm in vitro. *Nanomedicine (Lond.)* 10(10), 1539–1553 (2015).
10. Najafi A, Taheri AT, Mehdipour M, Martinez-Pastor F, Rouhollahi AA, Nourani MR. Improvement of post-thawed sperm quality in broiler breeder roosters by ellagic acid-loaded liposomes. *Poult. Sci.* 98(1), 440–446 (2019).
11. Kunzmann A, Andersson B, Thurnherr T, Krug H, Scheynius A, Fadeel B. Toxicology of engineered nanomaterials: focus on biocompatibility, biodistribution and biodegradation. *Biochim. Biophys. Acta.* 1810(3), 361–373 (2011).
12. Szebeni J. Complement activation-related pseudoallergy caused by liposomes, micellar carriers of intravenous drugs, and radiocontrast agents. *Crit. Rev. Ther. Drug Carrier Syst.* 18(6), 567–606 (2001).
13. Barkalina N, Jones C, Wood MJA, Coward K. Extracellular vesicle-mediated delivery of molecular compounds into gametes and embryos: learning from nature. *Hum. Reprod. Update.* 21(5), 627–639 (2015).
- **Review article discussing the clinical potential of using extracellular vesicles as a noninvasive alternative to infertility treatment.**
14. Raposo G, Stoorvogel W. Extracellular vesicles: exosomes, microvesicles, and friends. *J. Cell Biol.* 200(4), 373–383 (2013).
15. Colombo M, Raposo G, Théry C. Biogenesis, secretion, and intercellular interactions of exosomes and other extracellular vesicles. *Annu. Cell Dev. Biol.* 30, 255–289 (2014).
16. Osorio-Querejeta I, Carregal-Romero S, Ayerdi-Izquierdo A *et al.* MiR-219a-5p enriched extracellular vesicles induce OPC differentiation and EAE improvement more efficiently than liposomes and polymeric nanoparticles. *Pharmaceutics.* 12(2), 186 (2020).
17. Batrakova E, Kim MS. Using exosomes, naturally-equipped nanocarriers, for drug delivery. *J. Control. Release* 219, 396–405 (2015).
18. Kowal J, Tkach M, Théry C. Biogenesis and secretion of exosomes. *Curr. Opin. Cell Biol.* 29, 116–125 (2014).
19. Théry C, Witwer KW, Aikawa E *et al.* Minimal information for studies of extracellular vesicles 2018 (MISEV2018): a position statement of the International Society for Extracellular Vesicles and update of the MISEV2014 guidelines. *J. Extracell. Vesicles.* 7(1), 1535750 (2018).
- **Good laboratory guidelines by the International Society of Extracellular Vesicles for extracellular vesicle isolation, characterization and functional studies.**
20. Zhu X, Badawi M, Pomeroy S *et al.* Comprehensive toxicity and immunogenicity studies reveal minimal effects in mice following sustained dosing of extracellular vesicles derived from HEK293T cells. *J. Extracell. Vesicles* 6(1), 1324730 (2017).
21. Rosas LE, Elgamal OA, Mo X, Phelps MA, Schmittgen TD, Papenfuss TL. In vitro immunotoxicity assessment of culture-derived extracellular vesicles in human monocytes. *J. Immunotoxicol.* 13(5), 652–665 (2016).
22. Li J, Chen X, Yi J *et al.* Identification and characterization of 293T cell-derived exosomes by profiling the protein, mRNA and MicroRNA components. *PLoS One* 11(9), 0163043 (2016).

- **Proteomic and genomic analysis of exosomes derived from Human Embryonic Kidney 293T cells revealing no association with carcinogenic pathways.**
- 23. Watson DC, Yung BC, Bergamaschi C *et al.* Scalable, cGMP-compatible purification of extracellular vesicles carrying bioactive human heterodimeric IL-15/lactad-herin complexes. *J. Extracell. Vesicles.* 7(1), 1442088 (2018).
- 24. Liu Y, Li D, Liu Z *et al.* Targeted exosome-mediated delivery of opioid receptor Mu siRNA for the treatment of morphine relapse. *Sci. Rep.* 5, 17543 (2015).
- 25. El-Andaloussi S, Lee Y, Lakkhal-Littleton S *et al.* Exosome-mediated delivery of siRNA *in vitro* and *in vivo*. *Nat. Protoc.* 7(12), 2112–2126 (2012).
- **First research article to prove the *in vivo* and *in vitro* capabilities of HEK293T cell-derived exosomes for the loading of siRNA into murine brain tissue.**
- 26. Ruiss R, Jochum S, Mocikat R, Hammerschmidt W, Zeidler R. EBV-gp350 confers B-cell tropism to tailored exosomes and is a neo-antigen in normal and malignant B cells – a new option for the treatment of B-CLL. *PLoS One.* 6(10), 25294 (2011).
- 27. Sun D, Zhuang X, Xiang X *et al.* A novel nanoparticle drug delivery system: the anti-inflammatory activity of curcumin is enhanced when encapsulated in exosomes. *Mol. Ther.* 18(9), 1606–1614 (2010).
- 28. Alvarez-Erviti L, Seow Y, Yin H, Betts C, Lakkhal S, Wood MJ. Delivery of siRNA to the mouse brain by systemic injection of targeted exosomes. *Nat. Biotechnol.* 29(4), 341–345 (2011).
- 29. ELA S, Mager I, Breakefield XO, Wood MJ. Extracellular vesicles: biology and emerging therapeutic opportunities. *Nat. Rev. Drug Discov.* 12(5), 347–357 (2013).
- 30. You Y, Ikezu T. Emerging roles of extracellular vesicles in neurodegenerative disorders. *Neurobiol. Dis.* 130, 104512 (2019).
- 31. Ju Z, Ma J, Wang C, Yu J, Qiao Y, Hei F. Exosomes from iPSCs delivering siRNA attenuate intracellular adhesion molecule-1 expression and neutrophils adhesion in pulmonary microvascular endothelial cells. *Inflammation* 40(2), 486–496 (2017).
- 32. Wahlgren J, Karlson TDL, Brissert M *et al.* Plasma exosomes can deliver exogenous short interfering RNA to monocytes and lymphocytes. *Nucleic Acids Res.* 40(17), 130 (2012).
- 33. Ohno S, Takanashi M, Sudo K *et al.* Systemically injected exosomes targeted to EGFR deliver antitumor microRNA to breast cancer cells. *Mol. Ther.* 21(1), 185–191 (2013).
- 34. Tian Y, Li S, Song J *et al.* A doxorubicin delivery platform using engineered natural membrane vesicle exosomes for targeted tumor therapy. *Biomaterials.* 35(7), 2383–2390 (2014).
- 35. Piehl LL, Fischman ML, Hellman U, Cisale H, Miranda PV. Boar seminal plasma exosomes: effect on sperm function and protein identification by sequencing. *Theriogenology* 79(7), 1071–1082 (2013).
- **Research article showing the transfer of the 42 kDa actin protein from prostasomes into boar sperm.**
- 36. Du J, Shen J, Wang Y *et al.* Boar seminal plasma exosomes maintain sperm function by infiltrating into the sperm membrane. *Oncotarget* 7(37), 58832–58847 (2016).
- 37. Zhou W, Stanger SJ, Anderson AL *et al.* Mechanisms of tethering and cargo transfer during epididymosome-sperm interactions. *BMC Biol.* 17(1), 35 (2019).
- 38. Fernández-Gago R, Domínguez JC, Martínez-Pastor F. Seminal Plasma applied post-thawing affects boar sperm physiology. *Theriogenology* 80(4), 400–410 (2013).
- 39. Mogielnicka-Brzozowska M, Strzerek R, Wsilewska K, Kordan W. Prostasomes of canine seminal plasma – zinc-binding ability and effects on motility characteristics and plasma membrane integrity of spermatozoa. *Reprod. Domest. Anim.* 50(3), 484–491 (2015).
- 40. Aalberts M, Stout TA, Stoorvogel W. Prostasomes: extracellular vesicles from the prostate. *Reproduction* 147(1), 1–14 (2013).
- 41. Carpi A, Sabanegh E, Mechanick J. Controversies in the management of nonobstructive azoospermia. *Fertil. Steril.* 91(4), 963–970 (2009).
- 42. Shin D, Lo KC, Lipshultz LI. Treatment Options for the Infertile Male With Cancer. *J. Natl. Cancer Inst. Monogr.* 34, 48–50 (2005).
- 43. Dragovic RA, Collett GP, Hole P *et al.* Isolation of syncytiotrophoblast microvesicles and exosomes and their characterisation by multicolour flow cytometry and fluorescence Nanoparticle Tracking Analysis. *Methods.* 87, 64–74 (2015).
- 44. Carnell-Morris P, Tannetta D, Siupa A, Hole P, Dragovic R. Analysis of extracellular vesicles using fluorescence nanoparticle tracking analysis. In: *Extracellular Vesicles: Methods and Protocols, Methods in Molecular Biology (Volume 1660)* Kuo W, Jia S. (Eds). Humana Press, New York, NY Chapter 13 (2017).
- 45. Yeste M, Fernandez-Novell JM, Ramio-Lluch L *et al.* Intracellular calcium movements of boar spermatozoa during ‘in vitro’ capacitation and subsequent acrosome exocytosis follow a multiple-storage place, extracellular calcium-dependent model. *Andrology* 3(4), 729–747 (2015).
- 46. Jimenez I, Gonzalez-Marquez H, Ortiz R *et al.* Changes in the distribution of lectin receptors during capacitation and acrosome reaction in boar spermatozoa. *Theriogenology* 59(5–6), 1171–1180 (2003).
- 47. Ramio L, Rivera MM, Ramirez A *et al.* Dynamics of motile-sperm subpopulation structure in boar ejaculates subjected to “in vitro” capacitation and further “in vitro” acrosome reaction. *Theriogenology.* 69(4), 501–502 (2008).

48. Verstegen J, Iguer-Ouada M, Onclin K. Computer assisted semen analyzers in andrology research and veterinary practice. *Theriogenology* 57(1), 149–179 (2002).
49. Garner DL, Johnson LA. Viability Assessment of Mammalian Sperm Using SYBR-14 and Propidium Iodide1. *Biol. Reprod.* 53(2), 276–284 (1995).
50. Harrison RA, Ashworth PJ, Miller NG. Bicarbonate/CO₂, an effector of capacitation, induces a rapid and reversible change in the lipid architecture of boar sperm plasma membranes. *Mol. Reprod. Dev.* 45(3), 378–391 (1996).
51. Guthrie HG, Welch GR. Determination of intracellular reactive oxygen species and high mitochondrial membrane potential in Percoll-treated viable boar sperm using fluorescence-activated flow cytometry. *J. Anim. Sci.* 84(8), 2089–2100 (2006).
52. Webber J, Clayton A. How pure are your vesicles? *J. Extracell. Vesicles* 2, 19861 (2013).
53. Hoog JL, Lotvall J. Diversity of extracellular vesicles in human ejaculates revealed by cryo-electron microscopy. *J. Extracell. Vesicles* 4, 28680 (2015).
54. Poliakov A, Spilman M, Dokland T, Amling CL, Mobley JA. Structural heterogeneity and protein composition of exosome-like vesicles (prostasomes) in human semen. *Prostate* 69(2), 159–167 (2009).
55. Carpintero-Fernández P, Fafián-Labora J, O’Loughlen A. Technical advances to study extracellular vesicles. *Front. Mol. Biosci.* 4, 79 (2017).
56. Arienti G, Carlini E, Palmerini CA. Fusion of human sperm to prostasomes at acidic pH. *J. Membr. Biol.* 155(1), 89–94 (1997).
57. Schwarz A, Wennemuth G, Post H, Brandeburger T, Aumüller G, Wilhelm B. Vesicular transfer of membrane components to bovine epididymal spermatozoa. *Cell Tissue Res.* 353(3), 549–561 (2013).
58. Mulcahy LA, Pink RC, Carter DRF. Routes and mechanisms of extracellular vesicle uptake. *J. Extracell. Vesicles* 3, 24641 (2014).
59. Garcia Herreros M, Aparicio IM, Nunez I *et al.* Boar sperm velocity and motility patterns under capacitating and non-capacitating incubation conditions. *Theriogenology* 63(3), 795–805 (2005).
60. Boryshpolets S, Pérez-Cerezales S, Eisenbach M. Behavioral mechanism of human sperm in thermotaxis: a role for hyperactivation. *Hum. Reprod.* 30(4), 884–892 (2015).
61. Carlini E, Palmerini CA, Cosmi EV, Arienti G. Fusion of sperm with prostasomes: effects on membrane fluidity. *Arch. Biochem. Biophys.* 343(1), 6–12 (1997).
62. Caballero J, Frenette G, D’Amours O *et al.* Bovine sperm raft membrane associated Glioma Pathogenesis-Related 1-like protein 1 (GliPr1L1) is modified during the epididymal transit and is potentially involved in sperm binding to the zona pellucida. *J. Cell Physiol.* 227(12), 3876–3886 (2012).
63. Cross NL. Effect of cholesterol and other sterols on human sperm acrosomal responsiveness. *Mol. Reprod. Dev.* 45(2), 212–217 (1996).
64. Palmerini CA, Saccardi C, Carlini E, Fabiani R, Arienti G. Fusion of prostasomes to human spermatozoa stimulates the acrosome reaction. *Fertil. Steril.* 80(5), 1181–1184 (2003).
65. Bechoua S, Rieu I, Sion B, Grizard G. Prostasomes as potential modulators of tyrosine phosphorylation in human spermatozoa. *Syst. Biol. Reprod. Med.* 57(3), 139–148 (2011).
66. Arienti G, Carlini E, Saccardi C, Palmerini CA. Nitric oxide and fusion with prostasomes increase cytosolic calcium in progesterone-stimulated sperm. *Arch. Biochem. Biophys.* 402(2), 255–258 (2002).
67. García JC, Domínguez JC, Peña FJ *et al.* Thawing boar semen in the presence of seminal plasma: effects on sperm quality and fertility. *Anim. Reprod. Sci.* 119(1–2), 160–165 (2010).
68. Fernández-Gago R, Domínguez JC, Martínez-Pastor F. Seminal plasma applied post-thawing affects boar sperm physiology: a flow cytometry study. *Theriogenology* 80(4), 400–410 (2013).